FLUXONICS

NEWSLETTER

SUPERCONDUCTIVE ELECTRONICS IN EUROPE

N° 2 - August 2013

Edito

Since the early days of superconducting electronics, devices have been fabricated at the micrometre scale routinely, especially when applications were considered. Only the thicknesses of films, or tunnel barriers for Josephson junctions, were at the nanometre scale. With the fast rise of nanotechnologies, superconducting devices which are at the nanoscale in the three dimensions come to maturity for applications, enabled by nano-fabrication techniques and the understanding of their properties by physicists. They will be part of the next generation of applications, with larger complexity and capabilities. The next challenge is to know the ultimate limit of shrinkage, constrained by quantum macroscopic coherence, since speed and energy efficiency are not directly related to down-sizing for superconductors. A good news in these times of sharper budgets.

www.FLUXONICS.org

Technology highlight

Fabrication of self-shunted nano-SNIS Josephson junctions by a 3D Focused Ion Beam technique

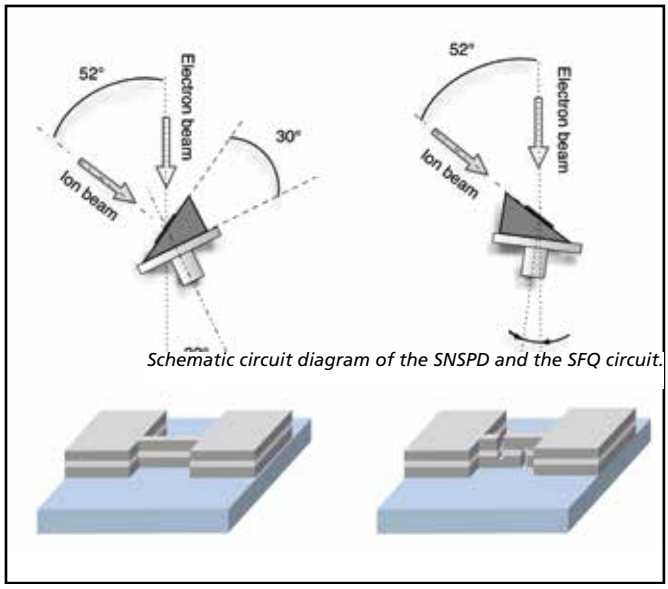

Schematic circuit diagram of the SNSPD and the SFQ circuit.

Fig. 1. Main steps for nano 3D SNIS JJs fabrication. The sample is positioned perpendicular (left) and then parallel (right) to the ion beam.

The challenges faced by quantum electronics and metrology are directing the new generations of devices towards smaller dimensions and higher levels of integration. Quantum information processes, single photon detection, nanoelectro-mechanical resonator systems, nanomagnetism and spintronics will benefit of improved performances achievable by nanofabrication processes. It is well-known for instance, that limitations on Superconducting Quantum Interference Devices (SQUIDs) sensitivity set by thermal noise can be reduced by lowering the inductance and capacitance of the device. Also in the circuits for Rapid Single Flux Quantum (RSFQ) a basic property such as the maximum clock frequency scales indirectly with dimensions. Furthermore, in the AC waveform generators, when a pulse driven source is employed, the maximum device size must be shorter than the minimal wavelength of the incident radiation.

Device downscaling must be pursued without affecting fundamental properties such as, for instance, the current-voltage (I-V) response of Josephson junctions (hysteretic or non-hysteretic behaviour). Rather, electrical parameters of the junctions, such as critical current, Ic and normal tunneling resistance, Rn must properly scale with dimensions. The downscaling is a technological challenge, since the merging of classical optical lithography with Reactive Ion Etching (RIE) and/or lift-off techniques to define the area entails an intrinsic and uncontrollable reduction of final dimensions.

In the following we report the early results on nano Nb/Al-AlOx/Nb SNIS (Superconductor - Normal metal - Insulator - Superconductor) junctions fabricated at INRIM exploiting an emerging technology for precision lithography.

The SNISs allow a proper I-V characteristic (overdamped or underdamped) to be designed and the main electrical parameters to be controlled through the "four-layered" structure engineering. Moreover, they exhibit a wide range of electrical parameters at liquid helium temperature, such as current densities, Jc ranging from 10^3 to 10^5 A/cm^2 and characteristic voltage, Vc up to 0.7 mV and the combination of these properties makes these junctions extremely appealing for digital applications and for programmable voltage standard.

SNIS junctions were fabricated by a three-dimensional Focused Ion Beam (3D FIB) etching technique, where the combination of Scanning Electron Microscope (SEM) and FIB revealed a powerful tool to create complex 3D nanostructures featuring good dimension control.

The FIB technique enables precise cutting material, selective material deposition, enhanced etching and end-point detection and has several advantages such as high sensitivity and resolution, high material removal rate, low forward scattering, and direct fabrication in selective area without using any etching mask.

The FIB lithography step was performed locating the specimen surface both perpendicular and parallel to the ion beam. First, a multilayered lamella was roughly narrowed up to 500 nm by a multi-step etching with a decreasing beam current, down to 100 pA (Figure 1, left). The impinging ions either implanted themselves or milled material from the surface of the sample, thus producing an amorphous layer and a buried implanted region within the surface. Consequently, to reduce these unwanted redeposition effects, the width of the lamella was further narrowed down to 390 nm, and hence the junction width was defined. Then, the sample was tilted and placed parallel to the ion beam trajectory. In this way two side cuts in the lamella were performed and the distance (390 nm) between them determines the junction length (Figure 1, right).

As previously mentioned, this highly energetic etching leads to spurious inclusions of implanted Ga+ ions and this event may influence the final electrical behavior of the junctions. Therefore, a standard anodization was performed to eliminate the unstructured layer and a further reduction of the effective JJs area down to about 280 x 280 nm was obtained. A SEM image of an angular view of a 3D SNIS junction fabricated by FIB is shown in Figure 2. The different layers of the Nb/Al-AlOx/Nb structure in the lamella may be easily recognized. In the inset of Figure 2, a scheme of the multilayered junction is represented with the flowing current through the barrier, labeled I.

In contrast to the SNIS fabrication process traditionally adopted where junctions are defined by optical lithography or Electron Beam Lithography (EBL) through the "window" process, the FIB processing requires neither resist masking, post-FIB wet or dry etching, nor resist removal. Accordingly, the entire device fabrication becomes more appealing due to the drastic reduction of fabrication steps.

The I-V response concerning the 3D SNIS junction with an effective area of about 280 x 280 nm and Ic of about 200 μA is shown in Figure 3, and the overdamping behavior is clearly maintained. This junction is characterized by Jc of 250 kA/cm^2, with Rn of 1.6 Ω and Vc of 320 μV. A measurement of the RF response of the junction to a microwave radiation at 70 GHz (Figure 4) clearly shows quantized steps up to n = 3. The inset in Figure 4 represents the n = 1 step (I = 90 μA) optimized by varying the RF power.
In conclusion, exploiting a 3D FIB etching technique the Nb/Al-AlOx/Nb SNIS junction area is easily controlled, still maintaining the fundamental properties of the junctions fabricated by other approaches. This method represents a promising technique for the fabrication of devices requiring mesoscopic tunneling junctions, alone or embedded into more complex circuits previously defined by standard optical lithography.

Natascia De Leo, Matteo Fretto and Vincenzo Lacquaniti
Istituto Nazionale di Ricerca Metrologica (I.N.Ri.M.)
Torino, Italy
Contact: n.deleo@inrim.it

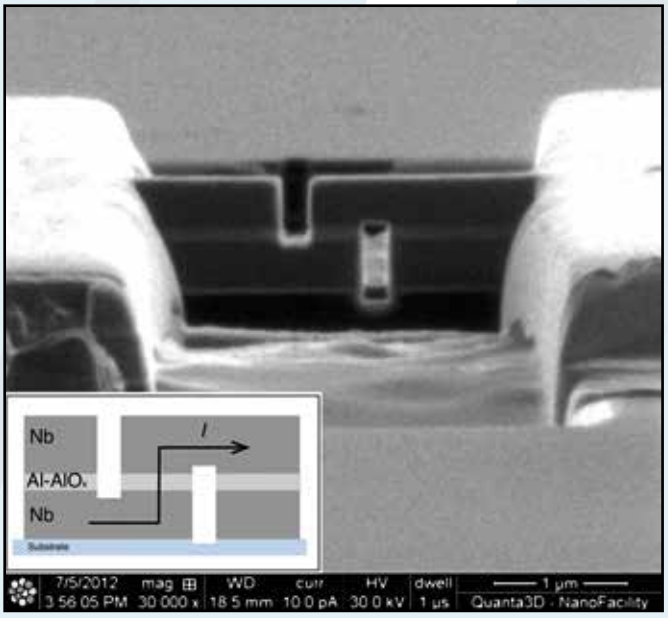

Fig. 2. A SEM image of a 3D SNIS junction. A scheme of the fabricated junction is represented in the inset, where the flowing current through the tunneling barrier is labeled I.

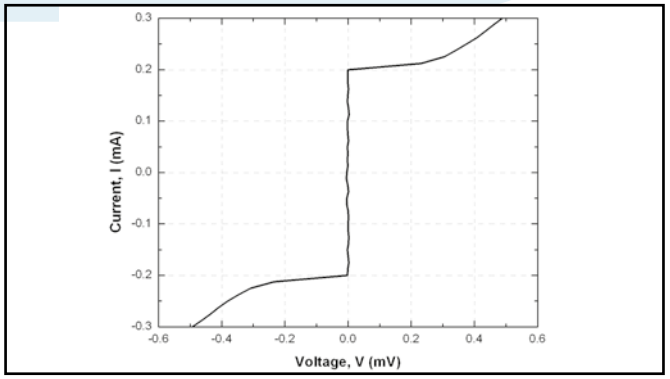

Fig. 3. Current–voltage characteristic referred to a 3D FIB SNIS junction with a Vc of 320 μV and Ic of 0.2 mA.

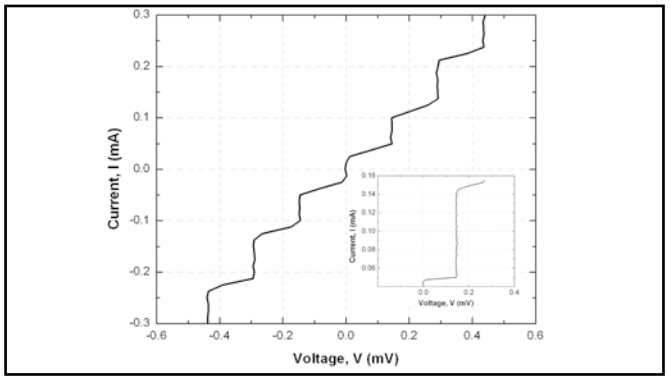

Fig. 4. Quantized voltage steps of a 3D FIB SNIS junction, measured at about 70 GHz, at 4.2 K. The n = 2 step is enhanced compared to the n = 1. The inset represents the optimized n = 1, with I of about 90 μA.

Focus

High-precision voltage measurements: superconductive electronics in metrology

FLUXONICS is a society dedicated to superconductive electronics, an extraordinary electronics making exciting applications possible. Some applications have successfully been established in metrology, the science of precision measurements. The main important representative of a metrological application is the Josephson voltage standard. Its most remarkable characteristic is that it is a quantum standard, which enables the reference of the volt (the unit of electrical voltage) only to physical constants and a frequency. Superconductivity as a macroscopic quantum effect plays here an essential role. This article focuses on recent developments and the current status of Josephson voltage standards at the Physikalisch-Technische Bundesanstalt (PTB) in Germany.

The discovery of the Josephson effect 50 years ago initiated a revolution for electrical voltage metrology. The 22-year-old graduate student Brian D. Josephson theoretically investigated the behaviour of two weakly coupled superconductors in 1962. He predicted the flow of superconducting currents through a so-called Josephson junction. High-frequency components of these currents at finite voltages can be phase locked by an external oscillator. Constant-voltage steps are generated by this phase lock, which forms the basis of all Josephson voltage standards. As an illustration, the generation of constant-voltage steps can be described by a specific transfer of flux quanta through the Josephson junction. The exceptional behaviour of Josephson junctions was experimentally confirmed shortly afterwards and has since become the basis of different applications of superconductive electronics. His discovery won Josephson a share of the 1973 Nobel Prize in Physics.

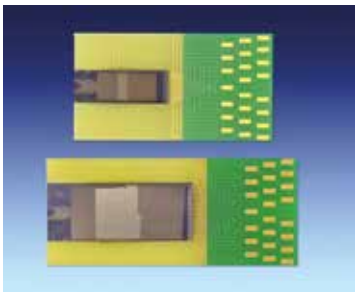

Photo of binary-divided series arrays: 1 V (top) and 10 V (bottom).

While a quantum voltage standard based on Josephson junctions is conceptually simple (a series array of Josephson junctions to increase the output voltage), about 50 years of developments were needed to progress from Josephson's idea to modern Josephson voltage standards for ac applications. This long period was caused by both the need for additional ideas and the required significant progress of the fabrication technology. The advanced current fabrication technology is a major prerequisite for modern Josephson voltage standards, as its main component is a highly integrated series array of Josephson junctions fabricated in thin-film technology under cleanroom conditions. The significant improvements made the progress possible from single junctions delivering a few millivolt at most to series arrays consisting of more than 10,000 or even 100,000 Josephson junctions delivering up to 20 V.

Josephson even mentioned the application of the Josephson effect for precise voltage measurements in his first paper. Constant-voltage steps are generated by microwave irradiation on Josephson junctions. The voltage U is determined by an integer n for the step number, the frequency f of the microwaves and the ratio of two fundamental constants (Planck's constant h and the elementary charge e): $Un = n \cdot (h / 2e) \cdot f$. As frequencies can be measured with very high precision by atomic clocks, Josephson junctions therefore enable the generation of high-precision voltages. A single junction operated at a microwave frequency of 70 GHz generates a voltage of 145 µV on the first step.

For roughly three decades, Josephson voltage standards were used for dc applications starting with single Josephson junctions for millivolts going up to highly integrated circuits containing up to 20,000 Josephson junctions and delivering 10 V. These conventional 10 V Josephson voltage standards are nowadays routinely used by some 50 laboratories worldwide for dc calibrations and related applications. They are now commercially available from two companies, Supracon in Germany and Hypres in the USA.

The increasing interest in highly precise ac voltages stimulated research activities in the mid 1990s to extend the use of measurement techniques based on Josephson junctions to ac applications and to develop corresponding tools. Conventional Josephson voltage standards are based on underdamped junctions, which cannot be used for ac applications. These junctions show a hysteretic current-voltage characteristic and a complete overlap of the constant-voltage steps causing an extremely multi-valued reference voltage at the relevant bias current. This behaviour prevents fast and specific switching between particular steps required for operation as ac voltage standards.

So-called overdamped Josephson junctions showing a non-hysteretic current-voltage characteristic enable the generation of single-valued constant-voltage steps under microwave irradiation. Different attempts for ac Josephson voltage standards have been suggested and partly realised since the mid 1990s. The two most successful types are based on binary-divided arrays and on pulse-driven arrays, respectively. Both types will be briefly introduced below.

Binary-divided arrays are the key component of programmable Josephson voltage standards. A series array of N junctions is divided into segments containing numbers of junctions belonging e.g. to a binary sequence. The

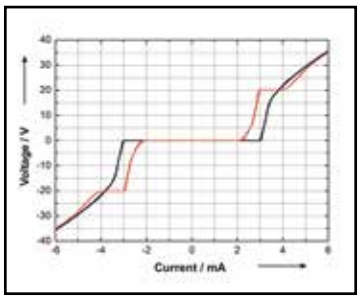

Current-voltage characteristic of a binary-divided 20 V array containing nearly 140,000 Josephson junctions without (black) and with 70 GHz (red) microwave irradiation.

junctions are operated on the zero and first order steps. Suitable external bias electronics enable the different segments of the series array to be rapidly switched on and off. Then, any number of junctions between –N and +N can be active at a given instant and add to the desired output voltage. The arrays act in principle as a digital-to-analogue converter. At PTB, programmable voltage standards are driven in the same frequency range around 70 GHz that is used for conventional Josephson voltage standards. 1 V circuits consisting of 8,192 junctions are operated in several laboratories worldwide. First 10 V circuits have besides been developed successfully at PTB containing about 70,000 junctions. The very robust fabrication technology needed for these large series arrays has been established by trilayer SNS junctions (layer sequence: Superconductor-Normal conductor-Superconductor).

Various applications like ac power standards, ac voltage calibrations, ac-dc transfer, and characterisation of analogue-to-digital converters have been suggested and demonstrated in part within the last decade. A significant contribution to the uncertainties of measurements using binary-divided arrays results from the transients which occur at the transition from one constant-voltage step to another, because the voltage is not determined by the Josephson equation during the transition.

Pulse-driven arrays avoid these limitations and enable the direct synthesis of ac voltages. They are operated by a train of short current pulses. These pulses effect the transfer of flux quanta through the Josephson junctions. Many pulses in time means the transfer of many flux quanta and therefore a high voltage. Fewer pulses in time reduce the transfer of flux quanta and thus the voltage. Arbitrary waveforms can be synthesised by adjusting the pulse train. The pulse drive makes the operation of these arrays more complex than that of arrays driven by sine-waves. A pulse repetition frequency up to 15 GHz is typically used. The output voltages are currently limited to the range below 0.3 V, because a parallel connection of microwave lines realised for conventional and binary-divided arrays is not possible for the pulse drive. Nevertheless, pulse-driven arrays enable the synthesis of arbitrary waveforms showing extremely pure frequency spectra. This type of ac Josephson voltage standard is therefore sometimes called the Josephson Arbitrary Waveform Synthesiser (JAWS).

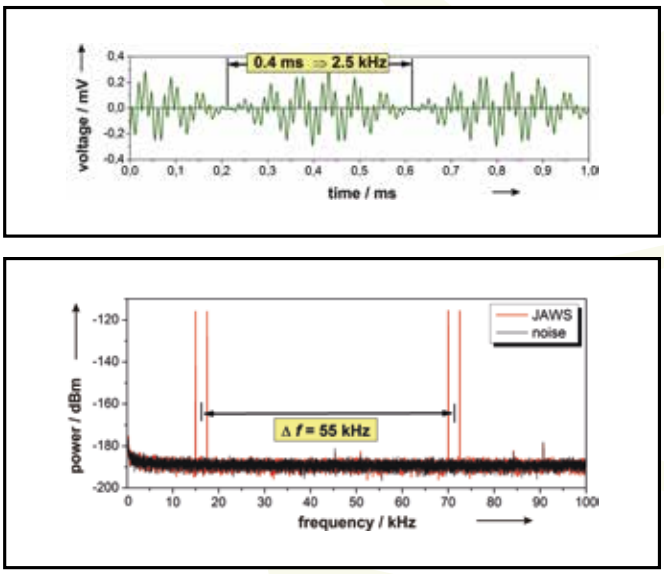

JAWS: synthesised 2 x 2 tone signal and corresponding frequency spectrum showing higher harmonics completely suppressed.

Both types of arrays for ac applications show advantages and drawbacks. While binary-divided arrays are available for output voltages up to 20 V (demonstrated by PTB), the output voltage of pulse-driven arrays is currently limited to root mean square (rms) values of about 0.275 V (realised at the National Institute of Standards and Technology (NIST), USA). On the other hand, pulse-driven arrays enable the synthesis of arbitrary waveforms with extremely pure frequency spectra. The frequency spectra of signals generated by binary-divided arrays contain in contrast a large amount of higher harmonics because of the operation principle as a digital-to-analogue converter. The use of sampling methods significantly reduces the influence of the transients for various applications of binary-divided arrays. Both types of voltage standards are currently in use depending on the respective application.

In spite of 50 exciting years, the development of Josephson voltage standards has not finished yet. The next step in the further research and development of Josephson junctions and their use for ac applications will partly be performed as tasks of two international research projects funded by the European Commission within the European Metrology Research Programme from mid 2013 till mid 2016.

Johannes Kohlmann
PTB Braunschweig, Germany
Contact: johannes.kohlmann@ptb.de

Further reading: R. Behr, O. Kieler, J. Kohlmann, F. Müller, and L. Palafox, "Development and metrological applications of Josephson arrays at PTB," Meas. Sci. Technol. 23 (2012) 124002 (19 pp).
Acknowledgement: Support of the PTB Josephson voltage standard team is gratefully acknowledged.

From laboratory research to SMEs

Operation and accuracy of an automated cryocooler-based 10 Volt Josephson Voltage Standard System

INTRODUCTION

Josephson voltage standard systems based on arrays of altogether 19,700 SIS Josephson tunnel junctions are commonly used as primary DC voltage standards. Applying them, secondary voltage standards as well as high precision digital voltmeters can be calibrated with the highest level of accuracy. Further developments are focused on a cryogenic-free operation [1, 2] and on programmable Josephson arrays [3, 4]. Because programmable Josephson arrays are difficult to manufacture at the 10 V level and in addition require an expensive control electronics the SIS Josephson voltage standard systems are still attractive, in particular due to the advantage of the availability of zero current steps.

The system was developed to be easy to use and to avoid a manual control of the Shaprio steps. In the following we describe the performance of the fully automated 10 Volt Josephson voltage standard system "supraVOLTcontrol" suitable for all DC voltage calibrations. A direct comparison to a helium based system showed an agreement of 1.3 nV at a relative uncertainty of 2×10^{-10}.

SETUP OF THE SYSTEM

The Josephson voltage standard system "supraVOLTcontrol" in the cryocooler version is shown in Figure 1. A pulse tube cooler delivered from the Transmit GmbH Giessen was used to establish the chip operating temperature of about 4K. The cryocooler itself produces a cooling power of about 180 mW at the cold stage. To reduce the thermal heat to the cold stage a 75 GHz dielectric microwave waveguide [2] were used for microwave transmission. The first and second stage of the cryocooler are thermally shielded and placed in a vacuum chamber. The chip itself is magnetically shielded by a cryoperm tube. This protection is required against earth magnetic field and the disturbances issued from the magnetic phase transition of the material located in the regenerator of the cryocooler. A box including LC filters was installed on the top of the cryocooler to reduce the noise level introduced by the bias electronics and the device under test. Careful grounding was necessary to reduce additional electrical noise from the compressor unit.

Figure 1: Photograph of "supraVOLTcontrol"

A good thermal coupling of the Josephson junction array (JJA) [5] to the cold stage is important in order to avoid a chip overheating. A thermal interface balances the different thermal expansion coefficients of the copper cold finger and the silicon chip.

Standard 4 K cryocoolers show temperature oscillations of about 0.2 K at the compressor cycling frequency. By the use of a nickel erbium plate, a material with a relative high thermal capacity at 4 K, the temperature oscillation could be reduced to 5 mK resulting in a stable operation.

The microwave with a frequency of 75 GHz is provided by a Gunn oscillator which is stabilized via the PLL of a 578B EIP counter. The microwave power is adjusted automatically to its optimum by a voltage controlled attenuator depending on the required Josephson output voltage.

The JJA is controlled by a µController electronics. A current source drives an AC current through the JJA and in parallel two 16 bit DACs as a voltage source adjust a course and fine voltage. In series to the voltage source a 100 Ω resistor is used for the step selection. With increasing microwave power Shapiro steps appear with a step number given by the voltage of the DACs and the resistor characteristic. The operating point of the JJA is found when the voltage drop at the resistor

[1] Y.-H. Tang, R.T. Hunt, R. Robertazzi, M.A. Fisher, J. Coughlin, R. Patt, E.K. Track, E. Potenziani, "Cryocooled Primary Voltage Standard System," IEEE Trans. Instrum. Meas., vol. 46, pp. 256-259, 1997.
[2] G. Wende, M. Schubert, T. May, L. Fritzsch, H.-G. Meyer, G. Thummes, Y. Kücükkaplan, L.M. Qiu, J. Kohlmann, J. Niemeyer, H. Hofmeister, and J. Scheerer, "Josephson Voltage Standard Circuit Operation with a Pulse Tube Cooler," IEEE Trans. Appl. Supercond., vol. 13, pp. 915-918, 2003.

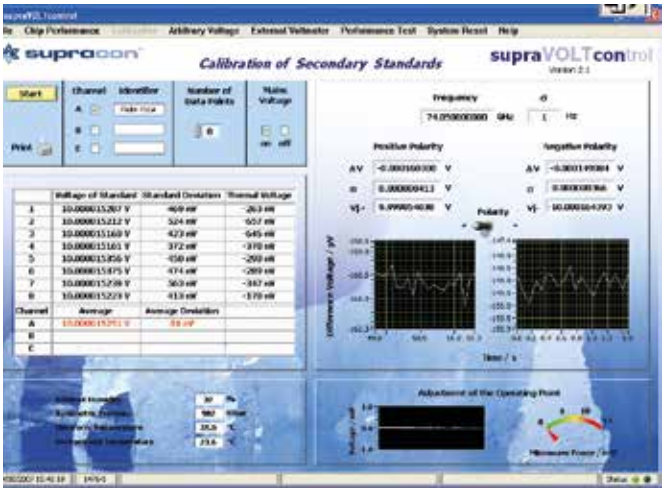

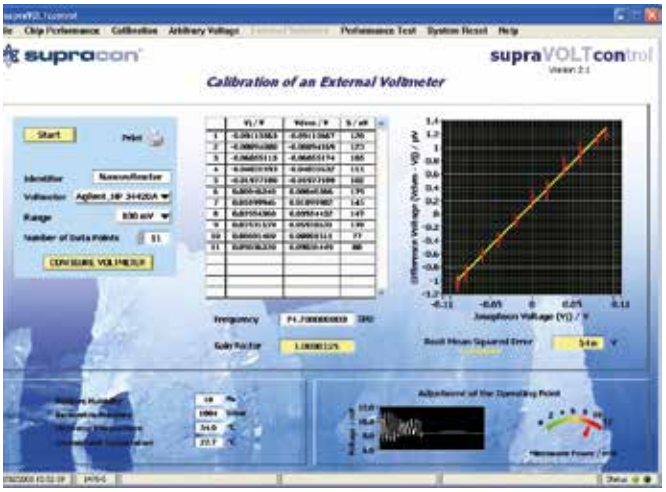

Figure 2: Graphic User Interface

becomes constant (± 100µV). The difference voltage of the JJA and a connected voltage standard is read out by a Keithley 2182A which acts as a null detector. In general the chosen voltage difference is smaller then 240 µV and 1 µV in the case of a direct comparison, respectively. A small difference voltage ensures a marginal influence of the gain error of the null detector. The JJA is disconnected from the bias electronics as well as from ground during the readout of the null detector. The system can automatically calibrate secondary voltage standards as well as the most common digital voltmeters which is shown in Figure 2, in a fast and highly accurate manner. For example the typical time for the calibrating a Fluke 732A with 20 points each in plus and minus polarity is only 30 s. For the measured DVMs the gain factor and nonlinearity will be specified.

DIRECT COMPARISON

A direct comparison between the cryocooler based system to a Liquid helium based system was carried out at a voltage level of 10 V in order to verify their accuracy. One system provided the Josephson voltage at 10 V and the second system measured this voltage. Both systems were driven at the same frequency of 74.7 GHz stabilized and phase locked to a GPS synchronized 10 MHz reference frequency. In order to avoid unwanted interferences of the systems during adjustment the Shapiro steps only one JJA was connected to its bias electronics and to ground, the other JJA was floating.

The results of the direct comparison are shown in Figure 3. Altogether eight measurements were made in about ten minutes. The error bars denote the standard deviation of the mean value of a single plus-minus-measurement with 20 points for each polarity. The result of the direct comparison is a difference of 1.3 nV at 10 V.

The combined standard uncertainty includes type A and type B components from both Josephson systems and is listed in Table 1. The experiments demonstrate an accuracy of the supraVOLTcontrol systems better than 2×10^{-10}.

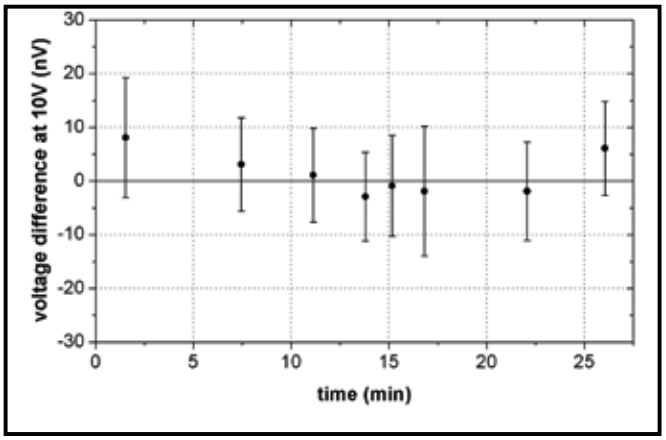

Figure 3: Direct Comparison of two Josephson Systems

QUANTITY	TYP	UNCERTAINTY
Measured Mean Voltage	A	1.44 nV
Frequency	B	1.0 nV
Leakage current	B	1.0 nV
Gain Error of Nanovoltmeter	B	0.2 nV
Total (RRS)	A and B	2.0 nV

Table 1: Uncertainty budget for a direct Josephson comparison

M. Starkloff, G. Wende, M. Meyer
Supracon AG, An der Lehmgrube 11, 07751 Jena, Germany, starkloff@supracon.com

S. Anders, H.-G. Meyer
Institute of Photonic Technologies (IPHT), P.O.Box 100239, D-07702 Jena, Germany

M. Schubert
Physikalisch-Technische Bundesanstalt (PTB), Bundesallee 100, 38116 Braunschweig, Germany

[3] C. A. Hamilton, S. P. Benz, C. J. Burroughs, and T. E. Harvey, "SNS Programmable Voltage Standard", IEEE Trans. Appl. Supercond., vol. 7, pp. 2472-2475, 1997.
[4] R. Behr, L. Palafox, G. Ramm, H. Moser, J. Melcher "Direct comparison of Josephson waveforms using an AC quantum voltmeter", IEEE Trans. Instrum. Meas., vol. 56, pp. 235-238, 2007.
[5] M. Schubert, T. May, G. Wende, L. Fritzsch, and H.-G. Meyer, "Coplanar strips for Josephson voltage standard circuits", Appl. Phys. Lett., vol. 79, pp. 1009-1011, 2001.

Thinking the next generation

New insight into voltage-biased SQUID operation

The need to optimally match the SQUID to the room-temperature preamplifier of the analog electronic readout, and to suppress of that preamp's noise has preoccupied the users from SQUID's early days [1]. Transformers and resonant circuits have been employed to improve impedance matching while the flux modulation technique was effective in the preamp noise suppression. Cryogenic amplifiers could also be used in special cases to reduce noise.

With the advent of multichannel SQUID systems in late 1980s and early 1990s, it became important to simplify the flux-locked loop readout and direct-coupled readout schemes were introduced. To suppress the preamp's noise they required some sort of additional feedback to enhance SQUID's dynamic resistance and ultimately $\partial V/\partial \Phi$. Two SQUID feedback schemes have been used in practice: the Additional Positive Feedback (APF) in current-biased SQUIDs, first proposed by Drung et al. [2], and the negative feedback Noise Cancellation (NC) scheme for voltage-biased SQUIDs first introduced by Kiviranta and Seppä of the VTT group [3]. The latter has been used in large multichannel systems fabricated by "Neuromag" for magnetoencephalography. However, both these schemes share a common disadvantage. They have narrow operating margins requiring either a rather tight SQUID parameter control in the fabrication process or an adjustable component, such as the FET transistor in the NC scheme.

Recently, Xie, Zhang et al. demonstrated for the voltage-biased SQUID a feedback circuit combining both voltage and current feedback, which they called SQUID Bootstrap Circuit (SBC) [4]. It has significantly improved operation margins but for a price of additional SQUID circuit complication so that only now the first planar integrated circuit version of SBC has been presented [5]. It is shown in Figure 1. However, in the process of its investigation Zhang and Liu realized that the voltage-biased SQUID can stably operate even when the Josephson junction Stewart-McCumber parameter βc exceeds 1 [5]. This is possible, because the low internal resistance of the voltage source shunts the junction resistance such that the effective $\beta ce \leq 1$.

The observation above led to a more systematic experimental investigation of the behavior of voltage-biased SQUIDs having nominal $\beta c \geq 1$. The now published results demonstrate that the voltage-biased SQUID with $\beta c \geq 1$, but $\beta ce < 1$, can have sufficiently high dynamic resistance, which improves matching sufficiently to largely suppress preamplifier's noise and no feedback circuit may be needed at all [6]. This would represent a dramatic simplification of the readout scheme.

In the published work [6] the SQUID parameter spreads were quite wide. The SBC could be employed as supplemental circuitry alleviating the need for tight manufacturing control. In any event, manufacturers of multichannel SQUID systems have now an additional strong incentive to attain such tight control as it would lead to the ultimately possible simplification of the readout scheme

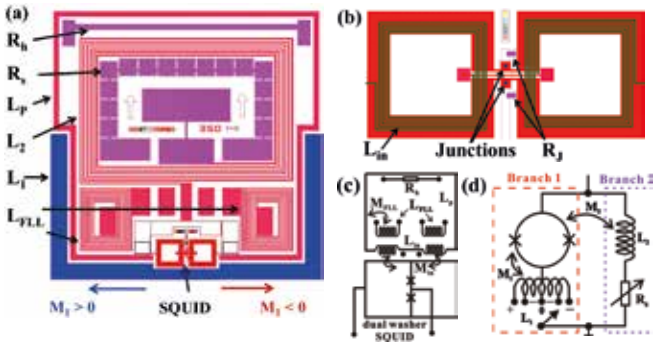

Figure 1. Layouts of (a) the SQUID chip with a size of 5 × 5 mm² and (b) the magnified dual-loop washer type SQUID with two opposite input coils with 4.5 turns each, also visible at the bottom of (a); (c) depicts the equivalent circuit of the SQUID magnetometer and (d) that of the bootstrap circuit [5].

Alex Braginski
Forschungszentrum Juelich GmbH, Germany
Contact: a.braginski@fz-juelich.de

Upcoming Events

EUCAS 2013, Genova, Italy / September 15-19, 2013

http://www.eucas2013.org

EUCAS is the biennial European Conference on Applied Superconductivity. The event brings together scientists, and industrial researchers and entrepreneurs, dealing in the Materials, Large Scale and Electronics aspects of applied superconductivity.

The RSFQ design FLUXONICS workshop, Ilmenau, Germany / September 25-28, 2013

http://www.ewh.ieee.org/tc/csc/europe/newsforum/pdf/A220

The 8th FLUXONICS workshop is directed to those who want to get familiar with aspects of design and simulation of superconductive electronic circuits and the development of emerging applications.

ISCM 2014, Antalya, Turkey – April 27-May 2, 2014

http://www.icsm2014.org

The Fourth International Conference on Superconductivity and Magnetism (ICSM 2014) will focus on advances in all major disciplines of superconductivity and magnetism.

ASC 2014, Charlotte, NC, USA - August 10-15, 2014

http://www.ascinc.org

The next edition of the Applied Superconductivity Conference (ASC 2014) will highlight the latest development in the field of superconductivity.

[1] D. Drung and M. Mück in „The SQUID Handbook" (J. Clarke and A.I. Braginski, Eds.) , vol. 1 Wiley-VCH, Weinheim 2004. [2] D. Drung, R. Cantor et al., Appl. Phys. Lett. 57 406 (1990) / [3] M. Kiviranta and H. Seppä, IEEE Trans. Appl. Supercond. 5 2146 (1995). [4] X. Xie, Yi Zhang et al., Supercond. Sci. Technol. 23 065016 (2010). [5] Yi Zhang, C. Liu et al. Supercond. Sci. Technol. 25 125007 (2012). [6] C. Liu, Yi Zhang et al., Appl. Phys. Lett. 101 222602 (2012).

Edited for the FLUXONICS Society by:
Pascal Febvre - IMEP-LAHC - CNRS UMR5130 - University of Savoie - France - Email: Pascal.Febvre@univ-savoie.fr - Phone: +33 47 975 8864